Prediction of the Bivariate Molecular Weight - Long Chain Branching Distribution in Highly Branched Polymerization Systems Using Monte Carlo and Sectional Grid Methods

Dimitrios Meimaroglou, Apostolos Krallis, Vassilis Saliakas, and Costas Kiparissides*

Department of Chemical Engineering, Aristotle University of Thessaloniki and Chemical Process Engineering Research Institute, P.O. Box 472, Thessaloniki, 54124, Greece

Received October 12, 2006; Revised Manuscript Received December 13, 2006

ABSTRACT: In the present work, an efficient Monte Carlo (MC) algorithm and a two-dimensional fixed pivot technique (FPT) are described for the calculation of the molecular weight distribution (MWD) for linear polymers (e.g., poly(methyl methacrylate), PMMA) and the bivariate molecular weight−long chain branching distribution (MW−LCBD) for highly branched polymers (e.g., poly(vinyl acetate), PVAc), produced in chemically initiated free-radical batch polymerization systems. The validity of the numerical calculations is first examined via a direct comparison of simulation results obtained by both methods with experimental data on monomer conversion and MWD for the free-radical MMA polymerization. Subsequently, the developed FPT and MC numerical algorithms are applied to a highly branched polymerization system (i.e., VAc). Simulation results are directly compared with available experimental measurements on M_n, M_w and B_n. Additional comparisons between the MC and the FP numerical methods are carried out under different polymerization conditions. In general, the 2-D FPT can provide very accurate predictions of the molecular weight averages and MWD for both linear and highly branched polymers in relatively short times but its numerical complexity requires special computational skills. On the other hand, the stochastic MC algorithm described in the present study is quite easy to implement but often requires large computational times, especially for highly branched polymers at high monomer conversions. It is important to point out that, to our knowledge, this is the first time that the joint (MW−LCB) distribution for branched polymers is calculated by two independent numerical methods via the direct solution of the governing population balance equations for both "live" and "dead" polymer chains.

Introduction

The elucidation of the molecular architecture of highly branched polymer chains in terms of the kinetic mechanism has been the subject of great number of theoretical and experimental studies. It is well-established that the molecular properties of polymers (e.g., molecular weight distribution, MWD, copolymer composition distribution, CCD, long chain branching distribution, LCBD, etc.) are directly related to their end-use properties (e.g., physical, chemical, mechanical, rheological, etc.). Hence, the ability to control accurately the molecular architecture of polymer chains in a polymerization reactor is of profound interest to the polymer industry.

A well-known approach for the calculation of the distributed polymer molecular properties (e.g., MWD, LCB, etc.) is the use of multivariate population balance equations[1] (PBE). In principle, based on the polymerization kinetic mechanism, one can derive dynamic PBEs to describe the time evolution of the "live" and "dead" polymer chains in a polymerization reactor. However, the total number of the resulting dynamic molar species balances is commonly of the order of hundreds or thousands equations. Consequently, the computational effort associated with the solution of the complete set of nonlinear differential equations is prohibitively high for most cases of interest. To deal with the above high dimensionality problem, several numerical methods have been proposed in the literature to reduce the infinite system of differential equations into a low-order system. These can be broadly classified into kinetic lumping methods,[2−5] polynomial expansion methods,[6] global orthogonal collocation,[7,8] method of moments,[9,10] "numerical fractionation" methods,[11−13] discrete weighted Galerkin,[14,15] orthogonal collocation on finite elements and sectional grid methods.[16] In general, the numerical methods mentioned above are computationally complex and require special mathematical skills. Commonly, a number of kinetic assumptions (e.g., the steady-state approximation for the "live" radical chains, absence of gel-effect, etc.) are made to simplify the numerical complexities associated with the solution of the governing PBEs. Note that the accuracy of the numerical solution is greatly dependent on the discretization of the chain-length domain which changes several orders of magnitude (e.g., 1 to 10^7).

An alternative approach to the above deterministic methods is the use of probabilistic tools (e.g., Monte Carlo simulations). Gillespie proposed a general stochastic simulation approach for chemically reacting systems.[17] On the basis of Gillespie's formulation, Yang and his co-workers developed Monte Carlo algorithms for the stochastic simulation of free-radical polymerization kinetics.[18−20] However, the formation of long-chain branches was never included in their implementations. Recently, a similar formulation was applied for the stochastic simulation of microemulsion polymerization.[21] Tobita and his co-workers followed a different stochastic approach (i.e., use of some known distributions for the polymer chains) to calculate the MWD and LCBD in free-radical highly branched polymerization systems.[22−25] However, they did not account for diffusion-controlled termination and propagation reactions and also assumed that the steady-state approximation for the "live" polymer chains holds true to simplify the numerical solution of the stochastic problem. The stochastic approach, while being very simple to implement, quite often requires long simulation times that can

* To whom correspondence should be addressed at the Department of Chemical Engineering, Aristotle University of Thessaloniki. E-mail: cypress@alexandros.cperi.certh.gr.

10.1021/ma0623439 CCC: $37.00
Published on Web 02/23/2007

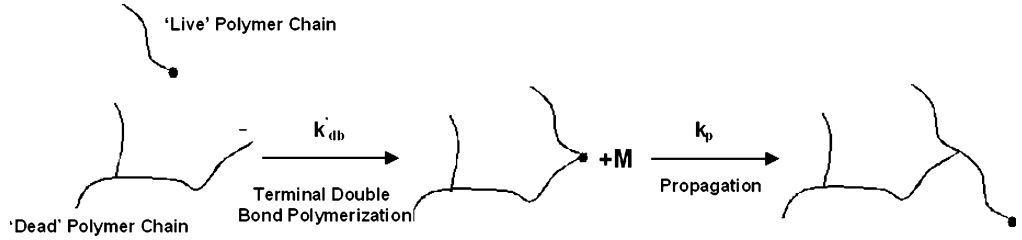

Figure 1. Formation of long chain branches via terminal double bond polymerization.

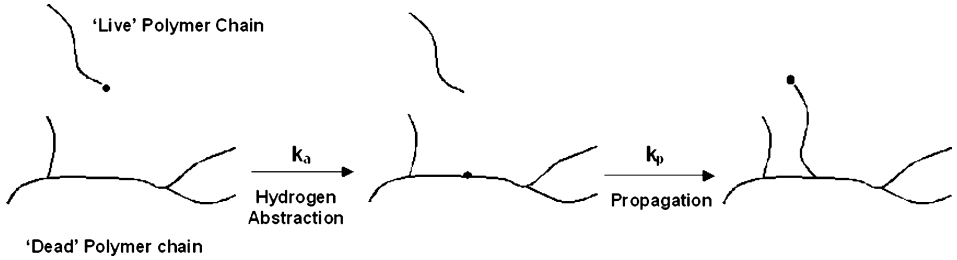

Figure 2. Formation of long chain branches via transfer to polymer reaction.

be a major drawback for the real-time simulation of an industrial polymerization process.

In the present work, two novel numerical approaches, namely, the two-dimensional fixed pivot technique (2-D FPT) and a stochastic Monte Carlo (MC) algorithm are described to calculate the MWD of "linear" polymers up to very high monomer conversions (e.g., 98%) and the bivariate (MW−LCB) distribution of highly branched polymers produced in free-radical batch polymerization reactors.

Kinetic Mechanism and Polymerization Rate Functions. In the present study, the following general kinetic mechanism was employed to describe the formation of both linear and highly branched polymers in chemically initiated free-radical polymerization systems.

Initiator decomposition:

$$I \xrightarrow{k_d} 2\mathrm{PR}^{\bullet} \tag{1}$$

Chain initiation:

$$\mathrm{PR}^{\bullet} + \mathrm{M} \xrightarrow{k_I} P_{0,1} \tag{2}$$

Propagation:

$$P_{\mathrm{b},n} + M \xrightarrow{k_p} P_{\mathrm{b},n+1} \tag{3}$$

Chain transfer to monomer:

$$P_{\mathrm{b},n} + M \xrightarrow{k_{fm}} D_{\mathrm{b},n} + P_{0,1} \tag{4}$$

Chain transfer to solvent:

$$P_{\mathrm{b},n} + S \xrightarrow{k_{fs}} D_{\mathrm{b},n} + P_{0,1} \tag{5}$$

Reaction with terminal double bond:

$$P_{\mathrm{b},n} + D_{\mathrm{r,m}} \xrightarrow{k_{db}} P_{\mathrm{b}+r+1,n+m} \tag{6}$$

Chain transfer to polymer:

$$P_{\mathrm{b},n} + D_{\mathrm{r,m}} \xrightarrow{k_{fp}} D_{\mathrm{b},n} + \mathrm{P}_{\mathrm{r}+1,m} \tag{7}$$

Termination by combination:

$$P_{\mathrm{b},n} + P_{\mathrm{r,m}} \xrightarrow{k_{tc}} D_{\mathrm{b}+r,n+m} \tag{8}$$

Termination by disproportionation:

$$P_{\mathrm{b},n} + P_{\mathrm{r,m}} \xrightarrow{k_{td}} D_{\mathrm{b},n} + \mathrm{D}_{\mathrm{r,m}} \tag{9}$$

where the symbols $P_{b,n}$ and $D_{\mathrm{b,n}}$ denote the respective "live" and "dead" polymer chains having "*b*" long chain branches and a total chain length equal to "*n*" . The above kinetic mechanism includes initiation and propagation reactions, termination by combination and disproportionation, molecular weight control reactions via transfer to monomer and solvent (chain transfer agent) and long chain branching formation via transfer to polymer and terminal double bond reactions.

Polymer chains having a terminal double bond, resulting from termination by disproportionation or/and transfer to monomer reactions, can react with "live" polymer chains to form long chain branches (see Figure 1).

Moreover, long chain branches can be formed via transfer to polymer reactions that involve the transfer of reactivity from a "live" polymer chain to a "dead" one. In the latter case, a hydrogen atom is first abstracted from the backbone of a "dead" polymer chain, leading to the formation of a "live" polymer chain having an internal radical center, and a "dead" polymer chain. Subsequent addition of monomer units to the internal radical center leads to the formation of a new long chain branch (see Figure 2). It should be noted that in the present study, a total rate constant of chain transfer to polymer was considered that involves both transfer mechenisms (i.e., transfer to the backbone, $-CH_2CH_2-$, and transfer to the side vinyl acetate group, CH_3COO-).

In the present study, in order to reduce the number of bivariate population balances to be solved numerically, it was assumed that the concentration of the "dead" polymer chains having a terminal double bond was some known fraction of the total number of "dead" polymer chains.[10] Thus, based on the postulated kinetic mechanism and assumptions, the following dynamic population balance equations for the "live", $P_{b,n}(t)$, and "dead", $D_{b,n}(t)$, polymer chains can be derived for a batch polymerization system:[1]

$$\frac{1}{V}\frac{\partial[VP_{b,n}(t)]}{\partial t} = r^{\mathrm{P}}_{\mathrm{b,n}}(t); \quad b = 0, 1, ..., N_{\mathrm{b}}; \quad n = 1, 2, ..., N_{\mathrm{n}} \tag{10}$$

$$\frac{1}{V}\frac{\partial[VD_{b,n}(t)]}{\partial t} = r^{\mathrm{D}}_{\mathrm{b,n}}(t); \quad b = 0, 1, ..., N_{\mathrm{b}}; \quad n = 1, 2, ..., N_{\mathrm{n}} \tag{11}$$

where $r^{\mathrm{P}}_{b,n}(t)$ and $r^{\mathrm{D}}_{b,n}(t)$ denote the corresponding net production rates for "live" and "dead" polymer chains, respectively. Their detailed functional forms are given by the following expressions:

Net formation rate of "live" polymer chains of length "n" with "b" branches:

$$\begin{aligned} r^{\mathrm{P}}_{\mathrm{b,n}}(t) = \{k_{\mathrm{I}}[\mathrm{PR}^{\bullet}][\mathrm{M}] + (k_{\mathrm{fm}}[\mathrm{M}] + k_{\mathrm{fs}}[S])\sum_{z=0}^{N_{\mathrm{b}}}\sum_{x=1}^{N_{\mathrm{n}}} P_{z,x}(t)\}\delta(n-1)\delta(b) + k_{\mathrm{p}}[\mathrm{M}][P_{b,n-1}(t) - P_{b,n}(t)] - (k_{\mathrm{fm}}[\mathrm{M}] + k_{\mathrm{fs}}[S])P_{b,n}(t) + \\ k_{\mathrm{fp}}nD_{b-1,n}(t)\sum_{z=0}^{N_{\mathrm{b}}}\sum_{x=1}^{N_{\mathrm{n}}} P_{\mathrm{z},x}(t) - k_{\mathrm{fp}}P_{\mathrm{b},n}(t)\sum_{z=0}^{N_{\mathrm{b}}}\sum_{x=2}^{N_{\mathrm{n}}} xD_{\mathrm{z},x}(t) - \\ k_{\mathrm{tc}}P_{\mathrm{b},n}(t)\sum_{z=0}^{N_{\mathrm{b}}}\sum_{x=1}^{N_{\mathrm{n}}} P_{\mathrm{z},x}(t) - k_{\mathrm{td}}P_{\mathrm{b},n}(t)\sum_{z=0}^{N_{\mathrm{b}}}\sum_{x=1}^{N_{\mathrm{n}}} P_{\mathrm{z},x}(t) - \\ k_{\mathrm{db}}P_{\mathrm{b},n}(t)\sum_{z=0}^{N_{\mathrm{b}}}\sum_{x=2}^{N_{\mathrm{n}}} D_{\mathrm{z},x}(t) + k_{\mathrm{db}}\sum_{z=0}^{b-1}\sum_{x=1}^{n-1} P_{\mathrm{z},n-x}(t)D_{\mathrm{b}-z-1,x}(t) \end{aligned} \tag{12}$$

Net formation rate of "dead" polymer chains of length "n" with "b" branches:

$$\begin{aligned} r^{\mathrm{D}}_{\mathrm{b,n}}(t) = (k_{\mathrm{fm}}[\mathrm{M}] + k_{\mathrm{fs}}[S])P_{b,n}(t) + \\ k_{\mathrm{fp}}P_{b,n}(t)\sum_{z=0}^{N_{\mathrm{b}}}\sum_{x=2}^{N_{\mathrm{n}}} xD_{\mathrm{z},x}(t) - k_{\mathrm{fp}}nD_{b,n}(t)\sum_{z=0}^{N_{\mathrm{b}}}\sum_{x=1}^{N_{\mathrm{n}}} P_{\mathrm{z},x}(t) - \\ k_{\mathrm{db}}D_{\mathrm{b},n}(t)\sum_{z=0}^{N_{\mathrm{b}}}\sum_{x=1}^{N_{\mathrm{n}}} P_{\mathrm{z},x}(t) + k_{\mathrm{td}}P_{\mathrm{b},n}(t)\sum_{z=0}^{N_{\mathrm{b}}}\sum_{x=1}^{N_{\mathrm{n}}} P_{\mathrm{z},x}(t) + \\ \frac{1}{2}k_{\mathrm{tc}}\sum_{z=0}^{b}\sum_{x=1}^{n-1} P_{\mathrm{z},x}(t)P_{\mathrm{b}-z,n-x}(t) \end{aligned} \tag{13}$$

where $\delta(n)$ is the Kronecker's δ function (i.e., $\delta(n) = 1$, if $n = 0$, and $\delta(n) = 0$, if $n \neq 0$). The symbols N_{b} and N_{n} denote the maximum number of branches and the maximum degree of polymerization, respectively.

The Monte Carlo Method. Assuming that the kinetics of a spatially homogeneous free-radical polymerization system can be approximated by a discrete stochastic process, a Monte Carlo (MC) algorithm can be developed to simulate its dynamic evolution. In the present study, following the original developments of Gillespie,[17] a simple and efficient algorithm was derived to describe the stochastic dynamic evolution of a chemically initiated free-radical batch polymerization system. The basic principles governing the proposed stochastic formulation are described next.

Let us first assume a spatially homogeneous mixture of N_{s} different molecular species, S_i, ($i = 1, 2, ..., N_{\mathrm{s}}$) of volume V. Let us also assume that X_i is the number of molecules of species "i" and that the different molecular species can interact with each other via N_{R} distinct chemical reactions. In general, the net formation rates for all the chemical reactions in the reacting system can be described by the following equation:

$$R_{\mathrm{j}} = k_{\mathrm{j}}\mathrm{X}^{\mathrm{c}}; \quad j = 1, 2, ..., N_{\mathrm{R}} \tag{14}$$

where k_j denotes the kinetic rate constant of the "jth" reaction and X^{c} is the total number of possible combinations of the molecules involved in a reaction step. That is, for a bimolecular chemical reaction of the type $S_1 + S_m \rightarrow S_n$ (k_{lm}), the net reaction rate will be equal to $R_j = k_{lm}\,X_l\,X_m$.

In Table 1, the MC calculated rates for all the reactions described by the general kinetic mechanism, eqs 1−9, are given.

Note that the time interval required for two successive reaction events to take place (i.e., the occurrence of the same reaction twice or the occurrence of two different chemical reactions of the kinetic mechanism) will be given by the following equation:

$$\Delta t = \left(\sum_{j=1}^{N_{\mathrm{R}}} R_j\right)^{-1}\ln(rn_{\mathrm{i}}^{-1}) \tag{15}$$

where rn_i is a randomly generated number from a uniform distribution in the range of [0,1]. To identify the reaction step, "j" , from the set of all possible reaction events ($j = 1, 2, ..., N_{\mathrm{R}}$) that will take place within the infinitesimal time interval ($t + \Delta t \rightarrow t + \Delta t + \mathrm{d}t$), the following equation is employed

$$\sum_{i=1}^{j-1} P_i < rn_k \leq \sum_{i=1}^{j} P_{\mathrm{i}} \tag{16}$$

where P_i denotes the probability for the occurrence of the "i" reaction and is given by

$$P_i = R_i/\sum_{z=1}^{N_R} R_{\mathrm{z}} \tag{17}$$

The MC simulation of all the chemical reactions described by the general polymerization kinetic scheme (see eqs 1−9) is straightforward. That is, after each time interval, Δt, individual polymer chains (either "live" or "dead") are randomly selected in order to react either with monomer molecules or other polymer chains, according to the defined reaction rates (see Table 1). Special attention must be paid to the MC simulation of the chain transfer to polymer reaction since, according to Table 1, the rate of consumption of "live" polymer chains for the production of "dead" polymer chains will be different from the rate of consumption of "dead" polymer chains for the production of "live" polymer chains. In this study, the chain transfer to polymer reaction was simulated by two different reaction steps (see Table 1), corresponding to two different reaction rates, R^1_{fp} and R^2_{fp}. Furthermore, the following probability criterion was implemented to account for the free-radical attacks on all chain-terminal carbon atoms in a "dead" polymer chain, $D_{r,m}$, that do not lead to the formation of a new long chain branch.

$$(m - r - 1)/m \geq rn_{\mathrm{i}} \tag{18}$$

where $(m - r - 1)$ denotes the total number of non-chain-terminal carbon atoms of the "dead" polymer chain, $D_{r,m}$. It should be noted that all the kinetic rate constants of the rate functions shown in Table 1 are expressed in terms of reacting molecules (i.e., molecules^{-1} min^{-1}) rather than in terms of concentration (i.e., L mol^{-1} min^{-1}). A detailed description of the MC algorithm, as applied in the present study, is shown in Figure 3.

In particular, the MC algorithm consists of the following steps:

Table 1. Monte Carlo Simulation of the Chemical Reactions and Their Respective Reaction Rates

reaction type	reaction rate	MC simulation algorithm
chain initiation (total reaction) $I \xrightarrow{k_d} 2P_{0,1}$	$R_i = k_d f I$	creation of two chains of type $P_{0,1}$ $I = I - 1$ $M = M - 2$
propagation $P_{b,n} + M \xrightarrow{k_p} P_{b,n+1}$	$R_p = k_p \lambda_0 M$	random selection of $P_{b,n}$ $P_{b,n} \rightarrow P_{b,n+1}$ $M = M - 1$
chain transfer to monomer $P_{b,n} + M \xrightarrow{k_{fm}} D_{b,n} + P_{0,1}$	$R_{fm} = k_{fm} \lambda_0 M$	random selection of $P_{b,n}$ creation of $D_{b,n}$ $P_{b,n} \rightarrow P_{0,1}$ $M = M - 1$
chain transfer to solvent $P_{b,n} + S \xrightarrow{k_{fs}} D_{b,n} + P_{0,1}$	$R_{fs} = k_{fs} \lambda_0 S$	random selection of $P_{b,n}$ Creation of $D_{b,n}$ $P_{b,n} \rightarrow P_{0,1}$ $S = S - 1$
reaction with terminal double bond $P_{b,n} + D_{r,m} \xrightarrow{k_{db}} P_{b+r+1,n+m}$	$R_{db} = k_{db} \lambda_0 \mu_0$	random selection of $P_{b,n}$ random selection of $D_{r,m}$ creation of $P_{b+r+1,n+m}$ removal of $P_{b,n}$ removal of $D_{r,m}$
chain transfer to polymer $P_{b,n} + D_{r,m} \xrightarrow{k_{fp}} D_{b,n} + P_{r+1,m}$	consumption of $P_{b,n}$ $R^1_{fp} = k_{fp} \lambda_0 \mu_1$ consumption of $D_{r,m}$ $R^2_{fp} = k_{fp} \lambda_0 \mu_0 m$	random selection of $P_{b,n}$ creation of $D_{b,n}$ removal of $P_{b,n}$ random selection of $D_{r,m}$ creation of $P_{r+1,m}$ if $(m - r - 1)/m \geq rn_i$ creation of $P_{r,m}$ if $(m - r - 1)/m < rn_i$ removal of $D_{r,m}$
termination by combination $P_{b,n} + P_{r,m} \xrightarrow{k_{tc}} D_{b+r,n+m}$	$R_{tc} = 0.5 k_{tc} \lambda_0(\lambda_0 - 1)$	random selection of $P_{b,n}$ random selection of $P_{r,m}$ creation of $D_{b+r,n+m}$ removal of $P_{b,n}$ removal of $P_{r,m}$
termination by disproportionation $P_{b,n} + P_{r,m} \xrightarrow{k_{td}} D_{b,n} + D_{r,m}$	$R_{td} = 0.5\, k_{td} \lambda_0(\lambda_0 - 1)$	random selection of $P_{b,n}$ random selection of $P_{r,m}$ creation of $D_{b,n}$ creation of $D_{r,m}$ removal of $P_{b,n}$ removal of $P_{r,m}$

Step 1: Initially, the MC simulation parameters are specified. This step includes the determination of the total polymerization time, t_p, and polymerization temperature, T, as well as the initial masses of monomer, $M(0)$, initiator, $I(0)$, and CTA, $S(0)$.

Step 2: Subsequently, a species sample is generated by dividing the initial volume of the system (i.e., monomer volume, V_0) by a factor, f. The mass of each species in the sample is then calculated and converted into respective initial numbers of molecules for monomer, initiator and CTA, (i.e., $M_s(0)$, $I_s(0)$, and $S_s(0)$).

Step 3: For each time interval, the kinetic rate constants of all the chemical reactions are calculated at the specified polymerization temperature, $T(t)$, and the current monomer conversion, $X(t)$, to account for the effects of diffusion-controlled termination and propagation reactions (i.e., gel- and glass-effect). Subsequently, all the chemical reaction probabilities are computed according to the rate functions shown in Table 1.

Step 4: From eq 15, the time interval, Δt, is then calculated and the chemical reaction that will take place after the elapse of the time interval is randomly determined, according to eq 16, through the selection of two unit-interval uniformly distributed random numbers.

Step 5: The identified chemical reaction is then simulated according to the respective step shown in Table 1.

Step 6: The values of the specified output variables (e.g., monomer conversion, leading moments of the MWD, etc.) are subsequently calculated.

Step 7: In the final step, the simulation time is advanced by the calculated time interval (i.e., $t = t + \Delta t$). The MC simulation is terminated when the total polymerization time has been reached (i.e., $t = t_p$). Otherwise, steps 3−7 are repeated.

From the MC simulation results, the number and weight-average molecular weights as well as the number and weight-average degrees of branching can be calculated using the following expressions:

Number-average molecular weight:

$$M_n = \left(\sum_{i=1}^{\mu_0} n_i^D/\mu_0\right) MW_m \tag{19}$$

Weight-average molecular weight:

$$M_n = \left(\sum_{i=1}^{\mu_0} (n_i^D)^2 / \sum_{i=1}^{\mu_0} n_i^D\right) MW_m \tag{20}$$

Number-average degree of branching:

$$B_n = \sum_{i=1}^{\mu_0} b_i^D/\mu_0 \tag{21}$$

Weight-average degree of branching:

$$B_w = \sum_{i=1}^{\mu_0} n_i^D\, b_i^D / \sum_{i=1}^{\mu_0} n_i^D \tag{22}$$

where n_i^D and b_i^D denote the respective total degree of polym-

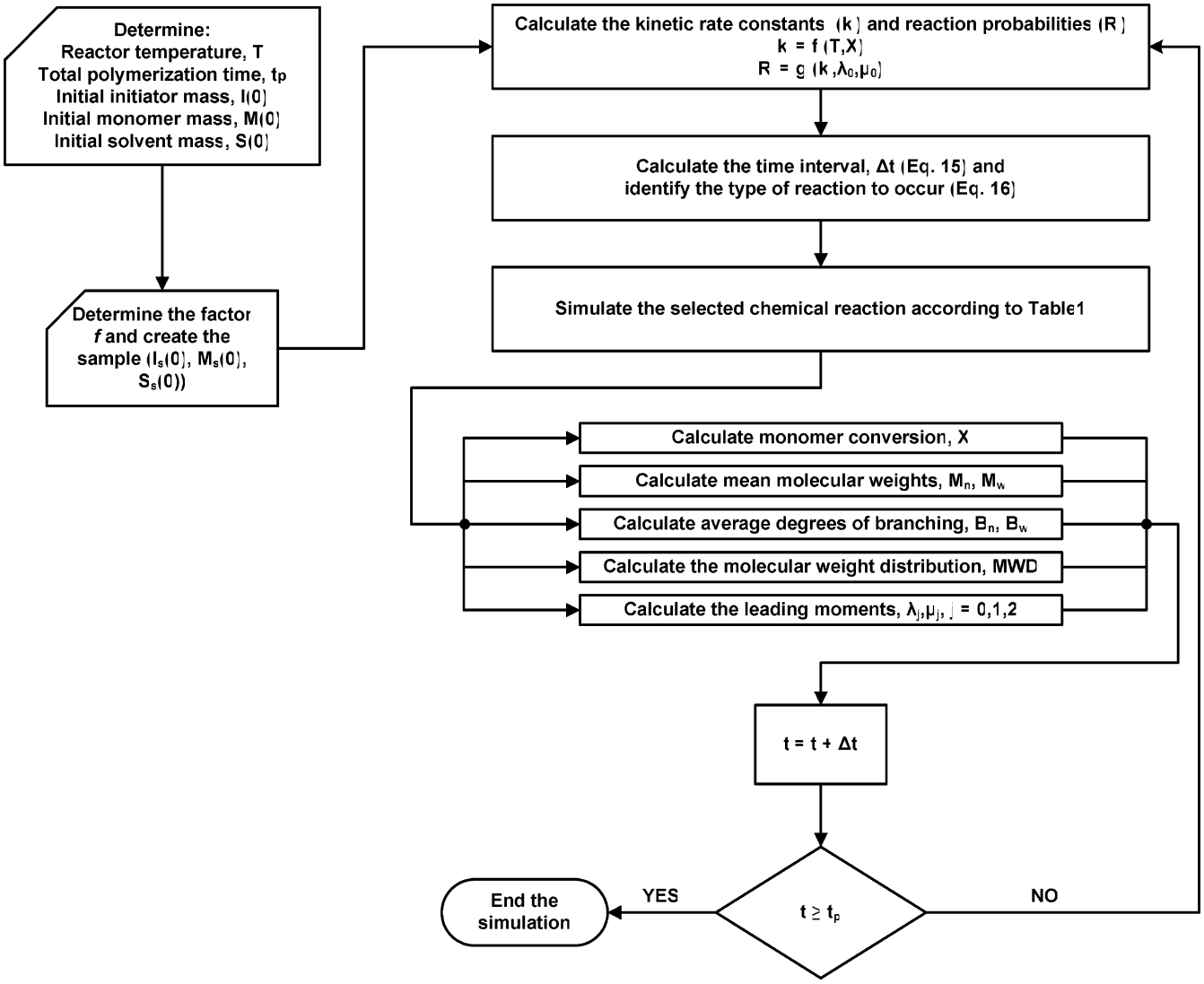

Figure 3. Schematic representation of the Monte Carlo algorithm.

erization and number of long chain branches for the "*i*th" "dead" polymer chain. μ_0 denotes the total number of "dead" polymer chains in the sample population.

To reconstruct the weight chain length distribution (WCLD), the total chain length domain is first discretized into a number of $N_{e,n}$ elements [$u_n(i)$; $i = 1, 2, ..., N_{e,n} + 1$]. Accordingly, the WCLD that corresponds to a specific value of LC branches, b_k, and the respective normalized total WCLD, W_f, are then calculated using the following expressions:

$$W = \sum_{\substack{j=1 \\ u_n(i)\le n_j^D<u_n(i+1) \\ \&b_j^D=b_k}}^{\mu_0} n_j^D/(u_n(i+1) - u_n(i)); \quad i = 1, 2, ..., N_{e,n} \tag{23}$$

$$W_f = [\sum_{\substack{j=1 \\ u_n(i)\le n_j^D<u_n(i+1)}}^{\mu_0} n_j^D/(u_n(i+1) - u_n(i))]/\sum_{j=1}^{\mu_0} n_j^D; \quad i = 1,2,...,N_{e,n} \tag{24}$$

The Fixed Pivot Technique. In the present study, a novel 2-D sectional-grid method was employed for solving the bivariate PBEs (see eqs 10 and 11). Specifically, the fixed pivot technique[26] (FPT) of Kumar and Ramkrishna was applied for calculating the dynamic evolution of the polymer chain populations (i.e., $P_{b,n}(t)$ and $D_{b,n}(t)$) in a free-radical batch polymerization reactor. Thus, the original system of PBEs was reduced to a finite number of discrete-continuous differential equations.

Following the original developments of Kumar and Ramkrishna,[26] the two-dimensional domain with respect to the number of LC branches per polymer chain and the total chain length (i.e., degree of polymerization) was discretized into a specific number of 2-D finite elements (Figure 4). Let $N_{e,b} + 1$ and $N_{e,n} + 1$ be the respective number of discrete points in the LC branches domain and in the total chain length domain. The symbols $u_b(j)(j = 1,2,...,N_{e,b} + 1)$ and $u_n(i)(i = 1,2,...,N_{e,n} + 1)$ denote the respective discrete values of LC branches and chain length. Let also $P(j,i,t)$ and $D(j,i,t)$ be the concentrations of the "live" and "dead" polymer chains in the center of a 2-D element defined by the four discrete points [($u_b(j)$, $u_n(i)$), ($u_b(j+1)$, $u_n(i)$), ($u_b(j)$, $u_n(i+1)$), (u_b(j+1), $u_n(i+1)$)] (see shaded area in Figure 4). Finally, let $b(j)$ and $n(i)$ be the corresponding discrete values for the number of LC branches and total chain length in the center of the above selected 2-D element. When new polymer chains are formed within the 2-D domain defined by the grid points [($b(j)$, $n(i)$), ($b(j+1)$, $n(i)$), ($b(j)$, $n(i+1)$), ($b(j+1)$, $n(i+1)$)] (see striped area in Figure 4), via termination by combination, transfer to polymer and terminal double bond polymerization, their concentrations are assigned

to the four neighboring grid points in such a way so that four selected moments (i.e., two in each domain) of the bivariate (MW−LCB) distribution are exactly preserved. On the other hand, polymer chains formed via initiation, transfer to monomer, transfer to solvent, or termination by disproportionation reactions do always correspond to the initially selected grid points.

From the application of the FPT to the bivariate PBEs, the following continuous-discrete rate functions for the "live" and "dead" polymer chains can be obtained:

Continuous-discrete rate for linear "live" polymer chains:

$$r_p(1,i,t) = 2\,f k_d[I]\delta(i-1) + k_{fs}[S]\Big(\sum_{l=1}^{N_{e,b}}\sum_{k=1}^{N_{e,n}} P(l,k,t)\Big)\delta(i-1) + k_{fm}[M]\Big(\sum_{l=1}^{N_{e,b}}\sum_{k=1}^{N_{e,n}} P(l,k,t)\Big)\delta(i-1) + k_p[M]\sum_{k=1}^{i} A(i,k)P(1,k,t) - k_p[M]P(1,i,t) - k_{fs}[S]P(1,i,t) - k_{fm}[M]P(1,i,t) - k_{fp}P(1,i,t)\sum_{l=1}^{N_{e,b}}\sum_{k=1}^{N_{e,n}} n(k)D(l,k,t) - k_{db}P(1,i,t)\sum_{l=1}^{N_{e,b}}\sum_{k=1}^{N_{e,n}} D(l,k,t) - k_{td}P(1,i,t)\sum_{l=1}^{N_{e,b}}\sum_{k=1}^{N_{e,n}} P(l,k,t) - k_{tc}P(1,i,t)\sum_{l=1}^{N_{e,b}}\sum_{k=1}^{N_{e,n}} P(l,k,t) \quad (25)$$

Continuous-discrete rate for branched "live" polymer chains:

$$r_p(j,i,t) = k_p[M]\sum_{k=1}^{i} A(i,k)P(j,k,t) - k_p[M]P(j,i,t) - k_{fs}[S]P(j,i,t) - k_{fm}[M]P(j,i,t) - k_{fp}P(j,i,t)\sum_{l=1}^{N_{e,b}}\sum_{k=1}^{N_{e,n}} n(k)D(l,k,t) + k_{fp}n(i)\left(\sum_{l=1}^{N_{e,b}}\sum_{k=1}^{N_{e,n}} P(l,k,t)\right)\left(\sum_{l=1}^{j} C(j,l)D(l,i,t)\right) - k_{db}P(j,i,t)\left(\sum_{l=1}^{N_{e,b}}\sum_{k=1}^{N_{e,n}} D(l,k,t)\right) - k_{td}P(j,i,t)\left(\sum_{l=1}^{N_{e,b}}\sum_{k=1}^{N_{e,n}} P(l,k,t)\right) + k_{db}\sum_{l=1}^{j}\sum_{q=1}^{j}\sum_{k=1}^{i}\sum_{m=1}^{i} B(i,k,m)\,T(j,l,q)\,P(l,k,t)\,D(q,m,t) - k_{tc}P(j,i,t)\left(\sum_{l=1}^{N_{e,b}}\sum_{k=1}^{N_{e,n}} P(l,k,t)\right) \quad (26)$$

Continuous-discrete rate for linear "dead" polymer chains:

$$r_D(1,i,t) = k_{fs}[S]P(1,i,t) + k_{fp}P(1,i,t)\sum_{l=1}^{N_{e,b}}\sum_{k=1}^{N_{e,n}} n(k)D(l,k,t) + k_{fm}[M]P(1,i,t) + k_{td}P(1,i,t)\sum_{l=1}^{N_{e,b}}\sum_{k=1}^{N_{e,n}} P(l,k,t) + k_{tc}\sum_{k=1}^{i}\sum_{m=k}^{i} B(i,k,m)\,P(1,k,t)\,P(1,m,t) - k_{fp}\,n(i)D(1,i,t)\sum_{l=1}^{N_{e,b}}\sum_{k=1}^{N_{e,n}} P(l,k,t) - k_{db}\,D(1,i,t)\sum_{l=1}^{N_{e,b}}\sum_{k=1}^{N_{e,n}} P(l,k,t) \quad (27)$$

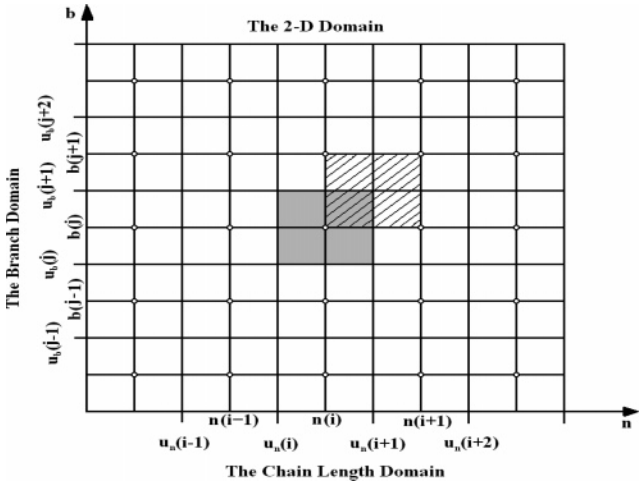

Figure 4. Representation of the 2-D discretization grid employed with the FPT.

Continuous-discrete rate for branched "dead" polymer chains:

$$r_D(j,i,t) = k_{fs}[S]P(j,i,t) + k_{fp}P(j,i,t)\sum_{l=1}^{N_{e,b}}\sum_{k=1}^{N_{e,n}} n(k)D(l,k,t) + k_{fm}[M]P(j,i,t) + k_{td}P(j,i,t)\sum_{l=1}^{N_{e,b}}\sum_{k=1}^{N_{e,n}} P(l,k,t) - k_{fp}\,n(i)D(j,i,t)\sum_{l=1}^{N_{e,b}}\sum_{k=1}^{N_{e,n}} P(l,k,t) - k_{db}D(j,i,t)\sum_{l=1}^{N_{e,b}}\sum_{k=1}^{N_{e,n}} P(l,k,t) + k_{tc}\sum_{l=1}^{j}\sum_{q=1}^{j}\sum_{k=1}^{i}\sum_{m=k}^{i} B(i,k,m)\,O(j,l,q)\,P(l,k,t)\,P(q,m,t) \quad (28)$$

where $j = 2, 3, ..., N_{e,b}$ and $i = 1, 2, ..., N_{e,n}$. Assuming that the zero and first moment of the bivariate distribution are preserved in each domain, the elements of the matrices $A(i,k)$, $B(i,k,m)$, $C(j,l)$, $T(j,l,q)$, and $O(j,l,q)$ can be calculated by the following expressions:

$$A(i,k) = \begin{cases} \dfrac{n(i+1)-n}{n(i+1)-n(i)} & n(i) \le n \le n(i+1) \\ \dfrac{n-n(i-1)}{n(i)-n(i-1)} & n(i-1) \le n \le n(i) \end{cases} \quad \text{and} \quad n = n(k)+1 \quad (29)$$

$$B(i,k,m) = \begin{cases} \dfrac{n(i+1)-n}{n(i+1)-n(i)} & n(i) \le n \le n(i+1) \\ \dfrac{n-n(i-1)}{n(i)-n(i-1)} & n(i-1) \le n \le n(i) \end{cases} \quad \text{and} \quad n = n(k)+n(m) \quad (30)$$

$$C(j,l) = \begin{cases} \dfrac{b(j+1)-b}{b(j+1)-b(j)} & b(j) \le b \le b(j+1) \\ \dfrac{b-b(j-1)}{b(j)-b(j-1)} & b(j-1) \le b \le b(j) \end{cases} \quad \text{and} \quad b = b(l)+1 \quad (31)$$

$$T(j,l,q) = \begin{cases} \dfrac{b(j+1)-b}{b(j+1)-b(j)} & b(j) \le b \le b(j+1) \\ \dfrac{b-b(j-1)}{b(j)-b(j-1)} & b(j-1) \le b \le b(j) \end{cases} \quad \text{and} \quad b = b(l)+b(q)+1 \quad (32)$$

$$O(j,l,q) = \begin{cases} \dfrac{b(j+1)-b}{b(j+1)-b(j)} & b(j) \le b \le b(j+1) \\ \dfrac{b-b(j-1)}{b(j)-b(j-1)} & b(j-1) \le b \le b(j) \end{cases} \quad \text{and} \quad b = b(l) + b(q) \quad (33)$$

where δ is the Kronecker's δ function.

Using the above calculated continuous-discrete rate functions one can derive a system of $[N_{e,b} \times N_{e,n}] \times 2$ continuous-discrete differential equations (DEs) to calculate the dynamic evolution of the bivariate number chain length distributions (NCLDs) of "live" and "dead" polymer chains:

$$\frac{1}{V}\frac{\partial[VP(j,i,t)]}{\partial t} = r_P(j,i,t); \quad j = 1, 2, ..., N_{e,b}; \quad i = 1, 2, ..., N_{e,n} \quad (34)$$

$$\frac{1}{V}\frac{\partial[VD(j,i,t)]}{\partial t} = r_D(j,i,t); \quad j = 1, 2, ..., N_{e,b}; \quad i = 1, 2, ..., N_{e,n} \quad (35)$$

By integrating the resulting system of DEs in time, the concentrations of the "dead" polymer chains at the grid points can be calculated. To reconstruct the WCLD that corresponds to a specific value of $b(j)$, the following approximation was employed:

$$W(j,i,t) = n(i)D(j,i,t)/(u_n(i+1) - u_n(i)); \quad i = 1, 2, ..., N_{e,n} \quad (36)$$

Accordingly, the normalized total weight chain length distribution, W_f, will be given by the sum of all distributions corresponding to the $N_{e,b}$ grid points of the LC branches domain:

$$W_f(i,t) = \frac{\sum_{l=1}^{N_{e,b}} [n(i)\, D(l,i,t)/(u_n(i+1) - u_n(i))]}{\sum_{l=1}^{N_{e,b}} \sum_{k=1}^{N_{e,n}} n(k)D(l,k,t)}; \quad i = 1, 2, ..., N_{e,n} \quad (37)$$

Note that both chain length and LC branch domains were discretized using a logarithmic rule. Typically, the chain length and branch domains were partitioned into 50 and 8 finite elements, respectively, leading to a total number of 800 discrete-continuous differential equations. To ensure that the selected number of elements was sufficient for the accurate reconstruction of the bivariate MW−LCB distribution a convergence criterion on the conservation of the total mass in the system was established.[16]

From the 2-D FPT simulation results, the number and weight-average molecular weights and the number and weight-average degrees of branching were calculated using the following equations:

Number-average molecular weight:

$$M_n = \left(\sum_{l=1}^{N_{e,b}} \sum_{k=1}^{N_{e,n}} n(k)D(l,k,t)\right) / \left(\sum_{l=1}^{N_{e,b}} \sum_{k=1}^{N_{e,n}} D(l,k,t)\right) MW_m \quad (38)$$

Weight-average molecular weight:

$$M_w = \left(\sum_{l=1}^{N_{e,b}} \sum_{k=1}^{N_{e,n}} n(k)^2 D(l,k,t)\right) / \left(\sum_{l=1}^{N_{e,b}} \sum_{k=1}^{N_{e,n}} n(k)\, D(l,k,t)\right) MW_m \quad (39)$$

Number-average degree of branching:

$$B_n = \left(\sum_{l=1}^{N_{e,b}} \sum_{k=1}^{N_{e,n}} b(l)\, D(l,k,t)\right) / \left(\sum_{l=1}^{N_{e,b}} \sum_{k=1}^{N_{e,n}} D(l,k,t)\right) \quad (40)$$

Weight-average degree of branching:

$$B_w = \left(\sum_{l=1}^{N_{e,b}} \sum_{k=1}^{N_{e,n}} n(k)\, b(l)\, D(l,k,t)\right) / \left(\sum_{l=1}^{N_{e,b}} \sum_{k=1}^{N_{e,n}} n(k)\, D(l,k,t)\right) \quad (41)$$

It should be pointed out that for linear polymer chains the above 2-D problem is reduced to a 1-D one. In this case, the complete set of discrete-continuous differential equations is significantly smaller (i.e., of the order of 100 differential equations). In fact, the continuous-discrete differential equations corresponding to the rate functions (eqs 25 and 27), need only to be integrated in time to calculate the dynamic evolution of the "live" and "dead" NCLDs.

Experimental Procedure

In order to validate the MC and FPT simulation results for the methyl methacrylate (MMA) free-radical batch polymerization system, a series of experiments were carried out in a 1 gallon (1 gallon = 4.55 L) stainless steel reactor equipped with a two-blade flat impeller. Apart from the agitated jacketed vessel, the reactor system comprised a heating−cooling unit, a monomer feed unit, a sampling unit, a vacuum unit, a reaction termination unit, and a supervisory process computer. Heating and cooling of the reaction mixture was achieved by controlling the flows of the two water streams (i.e., a hot and a cold one to the reactor jacket). The reactor was first purged with nitrogen prior to the addition of reactants (i.e., monomer water, initiator, etc.). At specific time intervals, samples were withdrawn from the reactor vessel for conversion and MWD measurements.

MMA (analytical grade from Aldrich, 99%) was used without any further purification. The stabilizer (PVA with a MW equal to 100 000 and a degree of hydrolysis equal to 86−89%, from Fluka) and the initiator (2,2′-Azobis(isobutyronitrile) AIBN, 98% from Aldrich) were used without any further purification as well. Polymerization experiments were carried out at 70 °C, whereas the agitation rate was kept constant. The monomer volume fraction and the PVA concentration were 0.40 and 0.2 g/L (based on the water volume), respectively. The initiator concentration was 0.3 wt % (with respect to the monomer).

Monomer conversion was measured gravimetrically. The MWD and the number- and weight-average molecular weights were measured by a gel permeation chromatographer, (GPC), model PL-GPC 210 plus viscometer. The GPC was equipped with two different detectors (for intrinsic viscosity and refractive index measurements).

Results and Discussion

Two free-radical polymerization systems, namely the free-radical polymerization of methyl methacrylate (MMA) and the free-radical polymerization of vinyl acetate (VAc), were employed as representative examples of linear (PMMA) and highly branched (PVAc) polymers. Numerical simulations using the two numerical methods (MC and FPT) were carried out for both systems, over a wide range of process conditions (i.e., temperature, initiator, monomer and CTA concentrations). The validity of the numerical calculations was first examined via a direct

Table 2. Kinetic Rate Constants for the Free-radical Polymerization System of MMA

$f_0 = 0.50$	*a*
$k_d = 6.32 \times 10^{16} \exp(-30600/RT)$(1/min)	*a*
$k_{p0} = 2.95 \times 10^7 \exp(-4353/RT)$ (m^3/kmolmin)	*a*
$k_{t0} = 11.88 \times 10^9 \exp(-701/RT)$ (m^3/kmol min)	*a*
$k_{fm}/k_p = 11.48 \times 10^3 \exp(-13020/RT)$	*a*
$k_{tc}/k_{td} = 8.956 \times 10^{-4} \exp(4500/RT)$	*a*
$k_{td} = k_t - k_{tc}$ (m^3/kmolmin)	*a*
$A = 0.168 - 8.21 \times 10^{-6} (T - 387.2)^2$; $B = 0.03$	*a*
$\theta_t = 1.935 \times 10^{-22} \exp(17580/T)/I_0$	*a*
$\theta_p = 7.4814 \times 10^{-16} \exp(13282/T)$	*a*

[a] Our own laboratory.

Table 3. Kinetic Rate Constants for the Free-radical Polymerization System of Vac

$f_i = 0.5$	*a*
$k_p = 4.2 \times 10^9 \exp(-6300/RT)$ (m^3/kmol min)	*a*
$k_{tc} = 1.62 \times 10^{12} \exp(-2800/RT)$ (m^3/kmol min)	*a*
$k_{td} = 0$	*b*
$k_{fm} = 4.957 \times 10^8 \exp(-10480/RT)$ (m^3/kmol min)	*c*
$k_{fp} = 5.177 \times 10^8 \exp(-11440/RT)$ (m^3/kmol min)	*c*
$k_{db} = 0.66\, k_p$	*a*
$k_d = 2.7 \times 10^{16} \exp(-30000/RT)$ (1/min)	*a*

[a] Hamer and Ray.[31] [b] Thomas.[27] [c] Our own laboratory.

comparison of simulation results obtained by both methods with experimental data on monomer conversion and MWD for the free-radical MMA polymerization. Subsequently, the developed FPT and MC numerical algorithms were applied to a highly branched polymerization system (i.e., VAc). Simulation results were directly compared with available experimental measurements on M_n, M_w and B_n, reported by Thomas.[27] Additional comparisons between the MC and the FP numerical methods were carried out under different polymerization conditions. The remarkable agreement between the results obtained by the two computational methods (i.e., the 2-D FPT and MC) provided strong evidence about the numerical accuracy of the proposed methods.

It is well-known that, in free-radical polymerization, the termination rate constant gradually decreases as the monomer conversion and, hence, the viscosity of the reaction mixture increases (i.e., gel-effect). To account for the diffusion-controlled phenomena appearing in the MMA polymerization, the works of Chiu et al.[28] (for gel-effect and glass-effect) and Achillias and Kiparissides[29] (for cage-effect) were employed. For the VAc polymerization, the original developments of Keramopoulos and Kiparissides[30] were followed. In Tables 2 and 3, the numerical values of kinetic rate constants for the two systems are reported.

In Figures 5 and 6, experimental measurements on MMA conversion and average molecular weights (i.e., M_n and M_w) of PMMA are compared with model predictions obtained by the two numerical methods (i.e., MC method and the 2-D FPT). It is evident that both methods display an excellent agreement with the experimental measurements.

In Figure 7, the molecular weight distributions calculated by the MC and FP methods are compared with the experimentally measured MWDs, at four different monomer conversions (i.e., 13%, 21%, 48%, and 94%). Apparently, there is a very good agreement between model predictions and experimental measurements.

In Figure 8, the effect of the sampling factor, *f*, on the reconstruction of the MWD calculated by the MC method is depicted. The calculated MWDs of PMMA correspond to a monomer conversion of 90% and a polymerization temperature of 80 °C. As can be seen, the calculated MWDs converge to a single distribution as the value of the sampling factor, *f*,

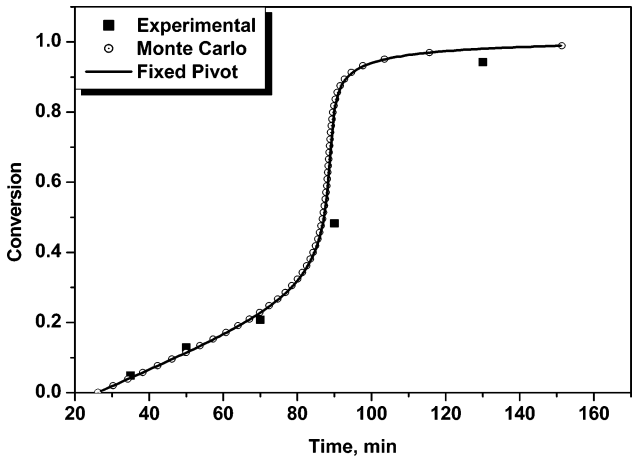

Figure 5. Calculated and experimental monomer conversion values for the free-radical MMA polymerization ($T = 70$ °C, $I_0 = 0.016$ kmol m^{-3}, $M(0) = 0.8$ kg).

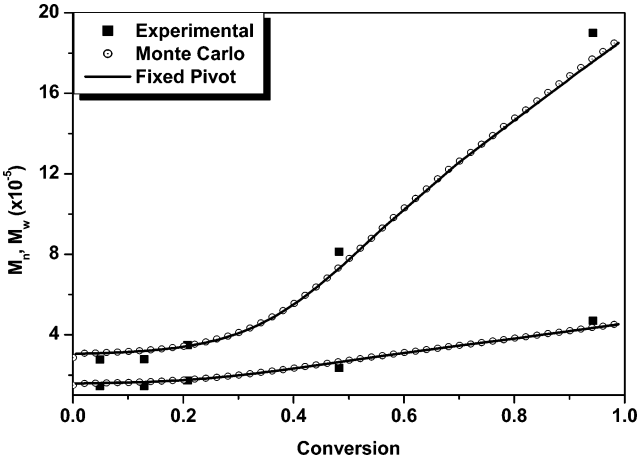

Figure 6. Calculated and experimental number and weight-average molecular weights ($T = 70$ °C, $I_0 = 0.016$ kmol m^{-3}, $M(0) = 0.8$ kg).

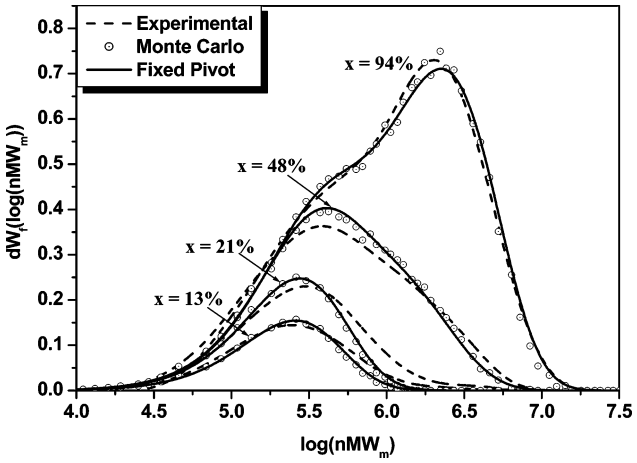

Figure 7. Calculated and experimental MWDs for the free-radical MMA polymerization at different monomer conversions ($T = 70$ °C, $I_0 = 0.016$ kmol m^{-3}, $M(0) = 0.8$ kg).

decreases. In the inset figure, the MC computational time is plotted with respect to the factor *f*. Apparently, as the value of *f* decreases the accuracy in the calculated MWD increases and so does the total simulation time.

In Figure 9, an additional comparison between the MWDs of PMMA calculated by the two methods at 62 °C is depicted. This comparison reveals the remarkable agreement between the results obtained by the two methods throughout the polymeri-

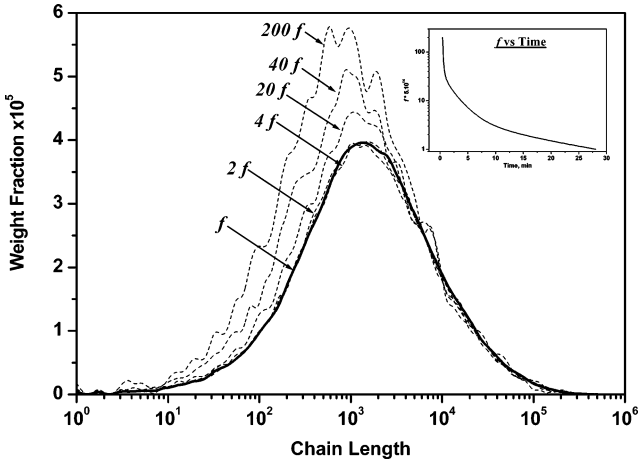

Figure 8. Effect of the sampling factor, f, on the convergence of the Monte Carlo algorithm (a) and on the required simulation time (b) (here: $f = 5 \times 10^{14}$) ($T = 80$ °C, $I_0 = 0.01$ kmol m^{-3}, $M(0) = 0.1$ kg).

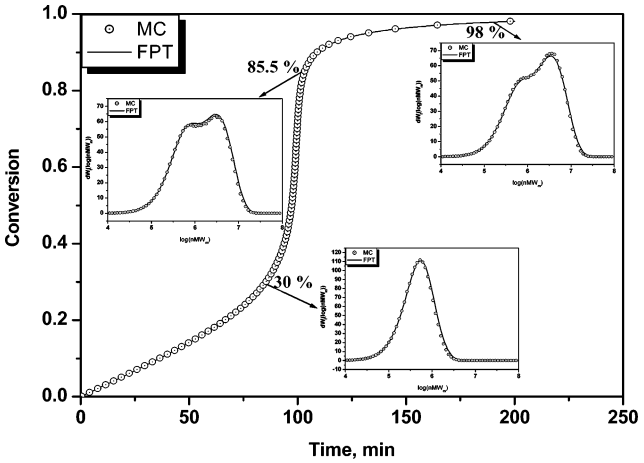

Figure 9. Monomer conversion and MWDs calculated by the Monte Carlo method and the 2-D FPT for the MMA free-radical polymerization system ($T = 62$ °C, $I_0 = 0.02$ kmol m^{-3}, $M(0) = 1.07$ kg).

zation process (i.e., up to very high monomer conversion, 98%). It should be emphasized that the commonly employed steady-state approximation for "live" radical chains was not applied in the present study. Moreover, it is the first time that MC simulations are carried out in the presence of diffusion-controlled reactions up to very high monomer conversions (i.e., the system becomes extremely stiff for integration) for branched polymerization systems.

In Figures 10−12, experimental measurements[27] on the number and weight-average molecular weights (i.e., M_n in Figure 10 and M_w in Figure 11) and number-average degree of branching (i.e., B_n in Figure 12) of PVAc, are compared with model predictions obtained by the two numerical methods (i.e., MC method and the 2-D FPT) at two different polymerization temperatures (i.e., 60 and 80 °C). Apparently, there is an excellent agreement between the simulation results obtained by the two numerical methods as well as with the experimental measurements for both polymerization temperatures.

In Figures 13 and 14, the joint (MW−LCB) distributions calculated by the MC algorithm are depicted for two monomer conversions (i.e., 50% and 90%), respectively. The polymerization was carried out at 60 °C. One can easily observe that long chain branching increases as the monomer conversion increases. The calculation of the joint (MW−LCB) distribution provides unique information on the distribution of branches at different chain lengths. To the best of our knowledge, it is the

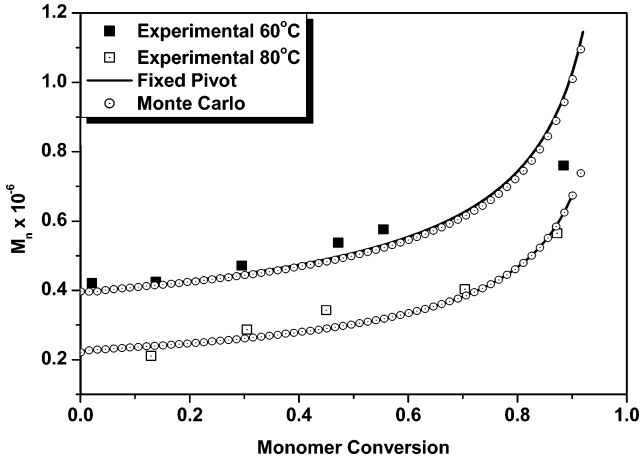

Figure 10. Calculated and experimental values of number-average molecular weight for the VAc free-radical polymerization ($T = 60$ °C, $I_0 = 5 \times 10^{-5}$ kmol m^{-3}, $T = 80$ °C, $I_0 = 1 \times 10^{-4}$ kmol m^{-3}, $M(0) = 0.1$ kg).

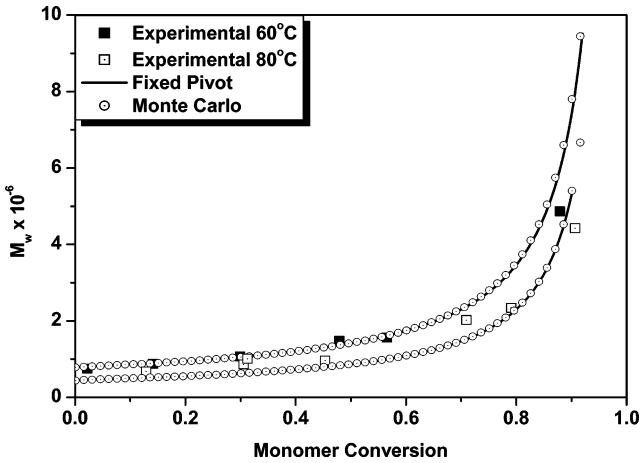

Figure 11. Calculated and experimental values of weight-average molecular weight for the VAc free-radical polymerization ($T = 60$ °C, $I_0 = 5 \times 10^{-5}$ kmol m^{-3}, $T = 80$ °C, $I_0 = 1 \times 10^{-4}$ kmol m^{-3}, $M(0) = 0.1$ kg).

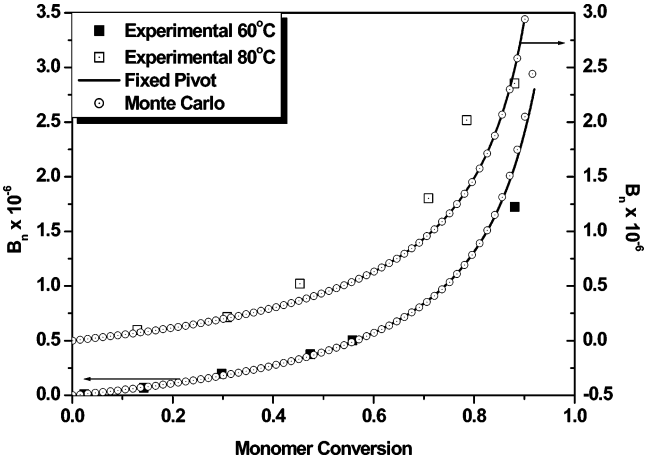

Figure 12. Calculated and experimental values of number-average degree of branching for the VAc free-radical polymerization ($T = 60$ °C, $I_0 = 5 \times 10^{-5}$ kmol m^{-3}, $T = 80$ °C, $I_0 = 1 \times 10^{-4}$ kmol m^{-3}, $M(0) = 0.1$ kg).

first time that the full bivariate MW−LCB distribution has been calculated for a highly branched polymerization system using the present MC formulation (i.e., including diffusion-controlled reactions and without the application of the quasi-steady state approximation for "live" polymer chains).

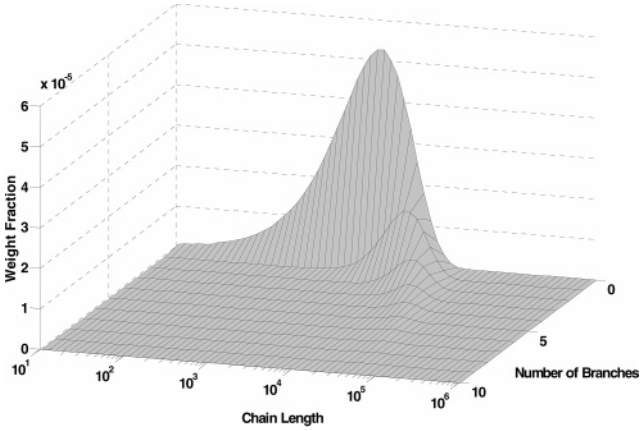

Figure 13. MC calculated bivariate MW−LCB distribution for the VAc free-radical polymerization, at a monomer conversion of 0.5 (T = 60 °C, I_0 = 0.0016 kmol m^{-3}, $M(0)$ = 0.1 kg).

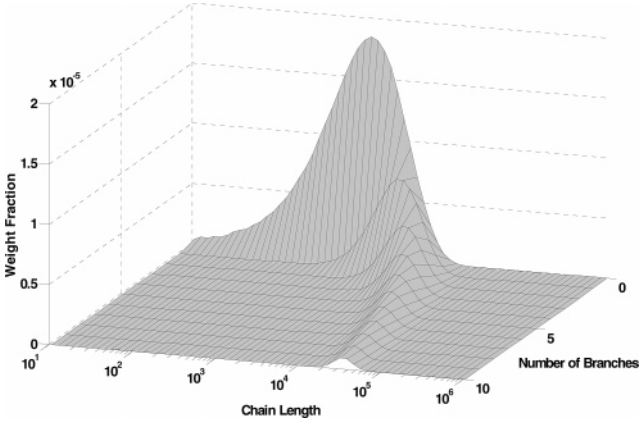

Figure 14. MC calculated bivariate MW−LCB distribution for the VAc free-radical polymerization ,at a monomer conversion of 0.9 (T = 60 °C, I_0 = 0.0016 kmol m^{-3}, $M(0)$ = 0.1 kg).

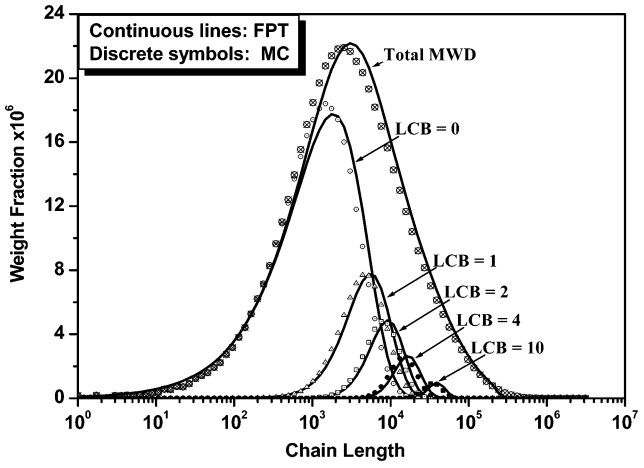

Figure 15. Comparison of the MC and the FPT calculated MWDs for linear and branched polymer chains of PVAc, at a monomer conversion of 0.9 and five different values of LCB (T = 60 °C, I_0 = 0.0016 kmol m^{-3}, $M(0)$ = 0.1 kg).

Finally, in Figure 15, the MWDs of PVAc, calculated by the FPT and MC method, are plotted for five different values of LCB content (i.e., 0, 1, 2, 4, and 10), at a monomer conversion of 90%. It can be seen that the distributions calculated by both numerical methods are in very good agreement at all values of LCB.

Conclusions

In this work, an efficient Monte Carlo algorithm and a 2-D fixed pivot technique were developed for the prediction of the MWD for linear polymers (PMMA) and branched polymers (PVAc), produced in chemically initiated batch free-radical polymerization systems. By a direct comparison of the numerical results obtained by the two methods with experimental measurements on monomer conversion, MWD and molecular weight averages the computational capabilities of the proposed methods were established. Extensive numerical simulations revealed the main advantages and disadvantages of the two numerical methods. In general, the implementation of the 2-D FPT is very complex and requires special computational skills. It was found that the calculated MWDs depend on the discretization of the chain length domain, thus, a careful selection of the number and size of the discrete elements in the FPT is required for the accurate reconstruction of the MWD. The MC stochastic method, on the other hand, is simpler in its implementation but requires higher computational times, especially for highly branched polymer systems at high monomer conversions.

Notation

B_n	number-average degree of branching
B_w	weight-average degree of branching
$b(i)$	grid point in the center of the "ith" element of the LC branches domain
b_i^D	number of LC branches for the "ith" "dead" polymer chain
$D_{b,n}$	concetration of "dead" polymer chains with "b" LC branches and a total chain length equal to "n" [kmol m^{-3}]
$D(j,i)$	concentration of the "dead" polymer chains in the center of the 2-D element defined by the four discrete points [($u_b(j)$, $u_n(i)$), ($u_b(j+1)$, $u_n(i)$), ($u_b(j)$, $u_n(i+1)$), and ($u_b(j+1)$, $u_n(i+1)$)] [kmol m^{-3}]
f	sampling factor in the MC algorithm
[I]	concentration of initiator [kmol m^{-3}]
I_0	initial concentration of initiator [kmol m^{-3}]
$I(0)$	initial mass of initiator [kg]
$I_s(0)$	initial number of molecules of initiator in the MC sample [molecules]
k_d	initiator decomposition rate constant [min^{-1}]
k_{db}	terminal double bond rate constant [m^3 kmol^{-1} min^{-1}]
k_{fm}	chain transfer to monomer rate constant [m^3 kmol^{-1} min^{-1}]
k_{fp}	chain transfer to polymer rate constant [m^3 kmol^{-1} min^{-1}]
k_{fs}	chain transfer to solvent (CTA) rate constant [m^3 kmol^{-1} min^{-1}]
k_I	initiation rate constant [m^3 kmol^{-1} min^{-1}]
k_p	propagation rate constant [m^3 kmol^{-1} min^{-1}]
k_{tc}	termination by combination rate constant [m^3 kmol^{-1} min^{-1}]
k_{td}	termination by disproportionation rate constant [m^3 kmol^{-1} min^{-1}]
[M]	concentration of monomer [kmol m^{-3}]
$M(0)$	initial mass of monomer [kg]
M_n	number-average molecular weight [kg kmol^{-1}]
$M_s(0)$	initial number of molecules of monomer in the MC sample [molecules]
M_w	weight-average molecular weight [kg kmol^{-1}]
MW_m	molecular weight of monomer [kg kmol^{-1}]
N_b	maximum number of branches
$N_{e,b}$	total number of elements on the LC branches domain
$N_{e,n}$	total number of elements on the chain length domain

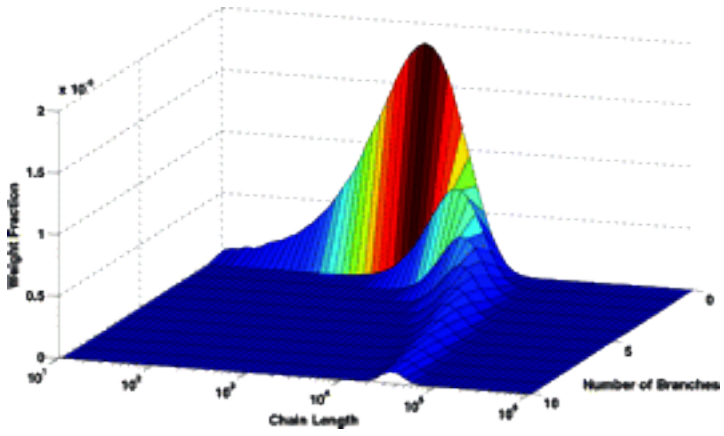
x 10^-4
2
1.5
1
0.5
0
Weight Fraction
10^1
10^2
10^3
10^4
10^5
10^6
Chain Length
0
5
10
Number of Branches

N_n maximum degree of polymerization

N_R total number of distinct chemical reactions that can take place in the MC sample

N_s number of different molecular species in the MC sample

$n(i)$ grid point in the center of the "*i*th" element of the chain length domain

n_i^D total degree of polymerization for the '*i*th' "dead" polymer chain

$P_{b,n}$ concetration of "live" polymer chains with "*b*" LC branches and a total chain length equal to "*n*" [kmol m^{-3}]

P_i MC probability for the occurrence of the "*i*th" chemical reaction

$P(j,i)$ concentration of the "live" polymer chains in the center of the 2-D element defined by the four discrete points [($u_b(j)$, $u_n(i)$), ($u_b(j+1)$, $u_n(i)$), ($u_b(j)$, $u_n(i+1)$), ($u_b(j+1)$, $u_n(i+1)$)] [kmol m^{-3}]

$[PR^\bullet]$ concentration of primary radicals [kmol m^{-3}]

R_i net formation rate of the '*i*th' chemical reaction in the MC algorithm [molecules min^{-1}]

$r_D(j,i)$ net production rate of "dead" polymer chains in the center of the 2-D element defined by the four discrete points [($u_b(j)$, $u_n(i)$), ($u_b(j+1)$, $u_n(i)$), ($u_b(j)$, $u_n(i+1)$), ($u_b(j+1)$, $u_n(i+1)$)] [kmol m^{-3} min^{-1}]

$r_P(j,i)$ net production rate of "live" polymer chains in the center of the 2-D element defined by the four discrete points [($u_b(j)$, $u_n(i)$), ($u_b(j+1)$, $u_n(i)$), ($u_b(j)$, $u_n(i+1)$), ($u_b(j+1)$, $u_n(i+1)$)] [kmol m^{-3} min^{-1}]

$r_{b,n}^D$ net production rate of "dead" polymer chains with "*b*" LC branches and a total chain length equal to "*n*" [kmol m^{-3} min^{-1}]

$r_{b,n}^P$ net production rate of "live" polymer chains with "*b*" LC branches and a total chain length equal to "*n*" [kmol m^{-3} min^{-1}]

rn_i randomly generated number from a uniform distribution in the range [0,1]

[S] concentration of chain transfer agent [kmol m^{-3}]

$S(0)$ initial mass of CTA [kg]

S_i type of the molecular species "i" in the MC sample

$S_s(0)$ initial number of molecules of CTA in the MC sample [molecules]

T polymerization temperature [°C]

t time [min]

t_p total polymerization time [min]

$u_b(i)$ left boundary of the '*i*th' element on the LC branches domain

$u_n(i)$ left boundary of the '*i*th' element on the total chain length domain

V volume of the dispersed phase [m^3]

V_0 initial volume of monomer [m^3]

X monomer conversion

X^c total number of possible combinations of the molecules involved in a reaction step, [molecules^a, where a is the order of the specific reaction step]

X_i number of molecules of species "*i*" in the MC sample [molecules]

Greek Letters

$\delta(n)$ Kronecker's δ function

Δt time interval in the MC algorithm [min]

λ_i "*i*th" moment of the "live" polymer chains

μ_i "*i*th" moment of the "dead" polymer chains

φ_m monomer volume fraction

φ_p polymer volume fraction

References and Notes

(1) Kiparissides, C. *J. Process Control* **2006**, *16*, 205−224.
(2) Crowley, T. J.; Choi, K. Y. *Ind. Eng. Chem. Res.* **1997**, *36*, 1419−1423.
(3) Crowley, T. J.; Choi, K. Y. *Ind. Eng. Chem. Res.* **1997**, *36*, 3667−3684.
(4) Crowley, T. J.; Choi, K. Y. *Chem. Eng. Sci.* **1998**, *53*, 2769−2790.
(5) Yoon, W. J.; Ryu, J. H.; Cheong, C.; Choi, K. Y. *Macromol. Theory Simul.* **1998**, *7*, 327−332.
(6) Tobita, H.; Ito, K. *Polym. React. Eng.* **1993**, *1*, 407−418.
(7) Canu, P.; Ray, W. H. *Comput. Chem. Eng.* **1991**, *15*, 549−564.
(8) Nele, M.; Sayer, C.; Pinto, J. C. *Macromol. Theory Simul.* **1999**, *8*, 199−213.
(9) Achilias, D. S.; Kiparissides, C. *J. Macromol. Sci.—Rev. Macromol. Chem. Phys.* **1992**, *C32*, 183−234.
(10) Baltsas, A.; Achilias, D.; Kiparissides, C. *Macromol. Theory Simul.* **1996**, *5*, 477−497.
(11) Teymour, F.; Campbell, J. D. *In Proceedings of the 4th International Workshop on Polymer Reaction Engineering*; Reichert, K. H., Moritz, H. U., Eds.; DECHEMA 127; VCH: Weinheim, Germany, 1992; p 149.
(12) Teymour, F.; Cambell, J. D. *Macromolecules* **1994**, *27*, 2460−2469.
(13) Pladis, P.; Kiparissides, C. *Chem. Eng. Sci.* **1998**, *53*, 3315−3333.
(14) Wulkow, M. *Macromol. Theory Simul.* **1996**, *5*, 393−416.
(15) Iedema, P. D.; Wulkow, M.; Hoefsloot, C. J. *Macromolecules* **2000**, *33*, 7173−7184.
(16) Krallis, A.; Kiparissides, C. *Chem. Eng. Sci.* **2006**, submitted for publication.
(17) Gillespie, D. T. *J. Phys. Chem.* **1977**, *81*, 2340−2361.
(18) Lu, J.; Zhang, H.; Yang, Y. *Macromol. Chem. Theory Simul.* **1993**, *2*, 746−760.
(19) He, J.; Zhang, H.; Yang, Y. *Macromol. Theory Simul.* **1995**, *4*, 811−819.
(20) He, J.; Zhang, H.; Chen, J.; Yang, Y. *Macromolecules* **1997**, *30*, 8010−8018.
(21) Nie, L.; Yang, W.; Zhang, H.; Fu, S. *Polymer* **2005**, *46*, 3175−3184.
(22) Tobita, H. *J. Polym. Sci. Phys. Ed.* **1993**, *31*, 1363−1371.
(23) Tobita, H. *J. Polym. Sci. Phys. Ed.* **1994**, *32*, 901−910.
(24) Tobita, H.; Hatanaka, K. *J. Polym. Sci. Phys. Ed.* **1995**, *33*, 841−853.
(25) Tobita, H.; Hatanaka, K. *J. Polym. Sci., Polym. Phys. Ed.* **1996**, *34*, 671−681.
(26) Kumar, S.; Ramkrishna, D. *Chem. Eng. Sci.* **1996**, *51*, 1311−1332.
(27) Thomas, S. Ph.D. Thesis, McMaster University, 1998.
(28) Chiu, W. Y.; Carratt, G. M.; Soong, D. S. *Macromolecules* **1983**, *16*, 348−357.
(29) Achilias, D. S.; Kiparissides, C. *Macromolecules* **1992**, *25*, 3739−3750.
(30) Keramopoulos, A.; Kiparissides, C. *Macromolecules* **2002**, *35*, 4155−4166.
(31) Hamer, J. W.; Ray, W. H. *Chem. Eng. Sci.* **1986**, *41*, 3083−3093.

MA0623439